MAGNETIC AND OPTICAL PROPERTIES OF MN-DOPED GAN THIN FILMS AND *P-I-N* DEVICES

M.L. Reed*, M.O. Luen, S.M. Bedair
Department of Electrical and Computer Engineering,
North Carolina State University, Raleigh, NC 27695-7911

M.J. Reed, F.E. Arkun, E.A. Berkman, N. A. El-Masry,
Department of Materials Science and Engineering,
North Carolina State University, Raleigh, NC 27695

J.M. Zavada
U.S. Army Research Office,
Durham, NC 27709

ABSTRACT

In this paper, we report on the growth and characterization of single crystal GaMnN thin films and *p-i-n* junction devices grown by metal-organic chemical vapor deposition (MOCVD). Single crystal GaMnN films were achieved by optimizing the growth temperature, growth rate and the Mn:Ga gas phase ratio. A growth window for obtaining single crystal $Ga_{1-x}Mn_xN$ with $0.006 \leq x \leq 0.023$ was found within a temperature range of $850ºC < T_G < 1040ºC$, as determined by transmission electron microscopy (Reed et al., 2001). Temperature dependent superconducting quantum interference device (SQUID) measurements confirmed the absence of superparamagnetism and spin glass behavior within the films and identified Curie temperatures between 228K and 500K for GaMnN.

It was found that the magnetic properties of MOCVD grown GaMnN are markedly affected by intentional introduction of donor or acceptor states into the film. Si or Mg co-doping of GaMnN films led to either ferromagnetic or paramagnetic behavior depending on the concentration. The magnetic properties of the GaMnN material system correlates with the Fermi level. Ferromagnetism was observed only when the Fermi energy level was near to the Mn energy band resulting in a partially occupied Mn energy level; a prerequisite for conduction within this band. The presence of the Fermi energy level within the Mn energy band allows the presence of carriers that mediate ferromagnetism. These results further confirm that the ferromagnetic properties result from a solid solution of Mn in the GaN and not from the presence of secondary phases, clusters, or precipitates, or secondary phases.

In addition to co-doping, the dependence of ferromagnetic properties of GaMnN films on carrier transfer across heterojunctions layers was also studied. The magnetic properties of GaMnN, as a part of GaMnN/GaN:Mg heterojunctions depend on the thickness of both the GaMnN film and the adjacent GaN:Mg layer. These results are explained based on the occupancy of the Mn energy band and how this occupancy is altered by carrier transfer at the GaMnN/GaN:Mg interface.

GaMnN *p-i-n* junction devices were also fabricated to study the effect of the magnetic properties on the I/V characteristics. These devices consist of *n*-GaN:Si/*i*-GaMnN/*p*-GaN:Mg layers grown by MOCVD. The carrier concentrations for the *n* and *p*-type layers are ~5 X 10^{18}/cm^3 and 1 X 10^{18}/cm^3 respectively. The GaMnN layer is approximately 0.1 – 0.2 μm thick with up to 1% Mn. The device pattern consisted of interdigitated fingers with a footprint of 400 μm X 400 μm. SQUID measurements of these devices show that the ferromagnetic properties were maintained during processing. Electroluminescence measurements for these devices showed visible emission at room temperature at ~ 410-430 nm. Eventually, it may be possible to combine electronic, magnetic, and optical functions on a single III-Nitride chip for novel applications.

1. INTRODUCTION

Current electronic device technology is separated primarily into two groups: semiconductor devices for processing and magnetic devices for data storage. The need for two different types of devices requires additional processing steps for integration, leading to more expensive and cumbersome components. In addition, device efficiency can be affected by electrical loss at interfaces and connections, as well as problems that may arise from stray electromagnetic radiation or heat dissipation. Obviously, these effects reduce the performance of the hybrid components on the soldier platform. By combining the use of both the charge and spin of the electron, a new class of electronic devices, capable of both data processing and storage, are possible. Such truly integrated

Report Documentation Page

Form Approved
OMB No. 0704-0188

1. REPORT DATE	2. REPORT TYPE	3. DATES COVERED
00 DEC 2004	**N/A**	**-**

4. TITLE AND SUBTITLE	5a. CONTRACT NUMBER
Magnetic And Optical Properties Of Mn-Doped Gan Thin Films And P-I-N Devices	5b. GRANT NUMBER
	5c. PROGRAM ELEMENT NUMBER
6. AUTHOR(S)	5d. PROJECT NUMBER
	5e. TASK NUMBER
	5f. WORK UNIT NUMBER
7. PERFORMING ORGANIZATION NAME(S) AND ADDRESS(ES) **Department of Electrical and Computer Engineering, North Carolina State University, Raleigh, NC 27695-7911; Department of Materials Science and Engineering, North Carolina State University, Raleigh, NC 27695**	8. PERFORMING ORGANIZATION REPORT NUMBER
9. SPONSORING/MONITORING AGENCY NAME(S) AND ADDRESS(ES)	10. SPONSOR/MONITOR'S ACRONYM(S)
	11. SPONSOR/MONITOR'S REPORT NUMBER(S)

12. DISTRIBUTION/AVAILABILITY STATEMENT
Approved for public release, distribution unlimited

13. SUPPLEMENTARY NOTES
See also ADM001736, Proceedings for the Army Science Conference (24th) Held on 29 November - 2 December 2005 in Orlando, Florida. , The original document contains color images.

14. ABSTRACT

15. SUBJECT TERMS

16. SECURITY CLASSIFICATION OF:			17. LIMITATION OF ABSTRACT	18. NUMBER OF PAGES	19a. NAME OF RESPONSIBLE PERSON
a. REPORT	b. ABSTRACT	c. THIS PAGE			
unclassified	**unclassified**	**unclassified**	**UU**	**8**	

Standard Form 298 (Rev. 8-98)
Prescribed by ANSI Std Z39-18

components would lead to improved efficiency and greater capability for the Future Combat System.

Initial efforts to realize spin dependent transport were performed using ferromagnetic metals as contacts in traditional semiconductor devices to facilitate spin polarized injection. However, these devices suffered from scattering at the metal/semiconductor interface, thus significantly reducing the spin injection to less than a few percent. This was attributed to the difference in the work function between the two materials. Ultimately, these studies led to a new type of material called dilute magnetic semiconductors (DMS) which were created by doping or alloying conventional semiconductors with a magnetic transition element, such as Mn. In DMS materials, a sizable number of nonmagnetic cations are replaced by magnetic ions to induce ferromagnetic behavior. Most researchers have focused on doping II-VI and III-As compound semiconductors with 3*d* transition elements. However, these compounds have low Curie temperatures, or paramagnetic behavior, making them impractical for room temperature application. The discovery and growth of Mn-doped III-Nitrides has been of significant interest since it is the first DMS to exhibit ferromagnetism at or above room temperature. Several groups have reported room temperature ferromagnetic (FM) properties of GaMnN grown by MOCVD and MBE (Sonoda et al., 2002; Thaler et al., 2002; Hori, 2002; Reed et al., 2001). Integrating this new technology with current III-Nitride devices, such as blue lasers and power transistors, should initially allow for more efficient devices with future innovations to include combined data processing and storage.

A great deal of emphasis has been placed on understanding the origin of the room temperature ferromagnetic behavior within GaMnN. In GaMnAs (a well-understood DMS), the Mn atoms form a relatively shallow acceptor level which provides localized magnetic moments and holes that mediate the magnetic interaction (Ohno, 1998; Koshihara et al., 1997). In GaMnN, the situation is quite different, since the Mn atoms form a deep energy level/band whose width depends on the Mn concentration (Korotkov et al., 2002; Sonoda et al., 2002; Thaler et al., 2004). Optical absorption measurements indicated the Mn energy band (E_{Mn}) is located 1.4 eV above the valence band edge of GaN as shown in figure 1 (Korotkov et al., 2002). The interaction of the Mn energy band with the valence band is limited and will not spin polarize the valence band. Therefore, the mechanism for ferromagnetic behavior in GaMnN cannot be the same as for GaMnAs. In this paper we show that ferromagnetism can only be achieved when the E_F resides within the Mn impurity band. Therefore, the location of the E_F will determine the occupancy of the Density of States (DOS) in this

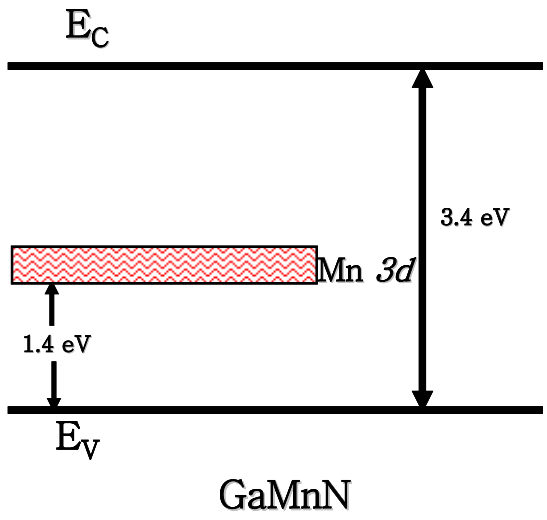

Fig. 1. Schematic showing the Mn energy band within GaMnN.

impurity band and thus the availability of carriers to mediate ferromagnetism. We demonstrate the dependence of the ferromagnetic properties on the Fermi level by co-doping GaMnN with *n*-type or *p*-type dopants. We also demonstrate how the magnetic properties can be altered via charge transfer across the GaMnN/GaN:Mg interface, and discuss preliminary data on several magnetic *p-i-n* junctions.

2. EXPERIMENTAL

GaN samples were grown by MOCVD on sapphire substrates using trimethylgallium (TMGa) and NH_3 precursors. The growth starts with a low temperature GaN buffer layer (500°C), followed by an undoped high-resistivity GaN film (~ 1 micron), and 0.2-0.5 micron layer of GaMnN, GaMnN:Si or GaMnN:Mg film. Silane and Mg-precursors (CP_2Mg) were used as *n*-type and *p*-type co-dopants. Mn was introduced during growth (growth temperature ~800-1000°C) using a metal-organic $(EtCP)_2Mn$ source with the bubbler at room temperature (20°C). The concentration of Mn in the GaMnN film was controlled by the partial pressure ratio of Mn:Ga in the gas phase.

X-ray diffraction (XRD) and high-resolution transmission electron microscopy (HRTEM) were used to observe the presence of any secondary phases in the Mn doped films used in this study. Secondary phases or atomic clusters were not detected by HRTEM and XRD for samples reported in this work (Reed et al., 2001, 2004). Secondary ion mass spectroscopy (SIMS) was used to determine the Mn concentration in GaMnN films. SIMS was also used to determine the Si and Mg concentration in GaMnN doped samples and *p-i-n* devices. The Mn

concentration depends on the Mn:Ga partial pressure ratio in the gas phase and ranges from 0.1 to 0.5 at%. A growth window for obtaining single crystal $Ga_{1-x}Mn_xN$ with $0.006 \leq x \leq 0.023$ was found within a temperature range of $850^oC < T_G < 1040^oC$, as determined by TEM and SIMS (Reed et al., 2001). The Mn concentration is measured to be ~10^{20} atoms/cm^3 for all the undoped, Si or Mg co-doped GaMnN samples and heterojunctions. A Mn-concentration of 0.5% was used in the *p-i-n* devices. The magnetic properties of undoped GaMnN, co-doped GaMnN:Si or GaMnN:Mg, heterojunctions and *p-i-n* devices were studied using superconducting quantum interference device (SQUID). The Hall measurement technique was used to determine the background carriers in all the samples. Electroluminescence and photoluminescence were used to characterize the *p-i-n* devices. Details regarding the specific growth conditions for each of the film types grown are discussed below.

3. RESULTS AND CONCLUSIONS

3.1 Fermi Position Study

GaMnN films grown for the Fermi position study all have a Mn-concentration of ~10^{20} atoms/cm^3. For Si doped GaMnN samples (GaMnN:Si), the silane flow was varied over several orders of magnitude using the double dilution technique. From the SIMS data, the maximum silicon concentration in GaMnN:Si for MOCVD grown films is ~$2x10^{20}$ atoms/cm^3. For GaMnN:Mg, the Mg concentration is found to range from $5x10^{19}$ to $2x10^{20}$ atoms/cm^3 (Reed et al., 2004). No variation in the Mn concentration (~10^{20}atoms/cm^3) of GaMnN films occurred because of co-doping by either Si or Mg.

Figure 2 shows the magnetization curves obtained by SQUID measurements for several Si doped GaMnN samples (one leg of the hysteresis loop for each sample is shown). The inset of figure 2 shows a full hysteresis loop with coercivity and saturation magnetization that is typical for ferromagnetic materials. The silicon concentration for the samples shown in figure 2 was controlled by varying the silane flow during the MOCVD growth. The silane flows for the samples in figure 2 are 0, 1.3, 6.7 and 84 nmol/min for samples a, b, c and d, respectively. The data in figure 2 indicates that increasing Si concentration reduces the magnetic strength of GaMnN films. In these GaMnN:Si samples, the Hall data was only measurable for the high Si doping level (84 nmol/min) giving n^+=10^{19}/cm^3. GaMnN:Si films with lower Si concentrations were found to be highly resistive. To further understand this material electronically, GaN:Si samples with the same Si concentrations used in this study were grown without Mn. GaN:Si with a silane flow of 84 nmol/min resulted in n^+=$2x10^{19}$/cm^3 which is similar to GaMnN:Si film grown under the same silane conditions. Consequently, Hall measurements of GaN:Si films grown using the same low and moderate silane flow without Mn resulted in n=$5x10^{18}$ and $7x10^{18}$/cm^3, respectively. Although these results differ from GaMnN:Si films with the same silane flow, it is expected that the same levels of doping are present.

The experimental data for GaMnN:Si can be explained based upon the location of the Fermi level (E_F) within this material system. The location of the Fermi level will determine the occupancy of the DOS in this Mn

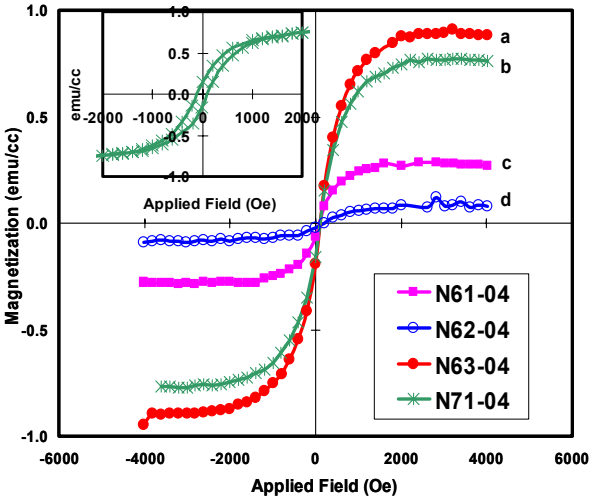

Fig. 2. The effect of Si concentration on the magnetic properties of GaMnN:Si; keeping the Mn concentration in the films at 10^{20} atoms/cm^3. SQUID measurements for (a) GaMnN-undoped, (b) GaMnN:Si (Si=2 nmole/min), (c) Si=6.8 nmole/min, (d) Si=84 nmole/min. The inset shows the full hysteresis curve with coercivity typical of ferromagnetic materials.

impurity band and the availability of carriers to mediate the Mn-Mn exchange magnetic interaction. In GaMnN films grown under the proper growth conditions, the Fermi level lies within or close to the Mn impurity band. When the Fermi position is such that there is a partial occupancy of electrons and holes in this Mn impurity band, ferromagnetic behavior occurs as shown in figure 2a. In the case of n^+ GaMnN:Si (n+ ~$2x10^{19}$ /cm^3), it is expected that E_F is close to the conduction band. Therefore, the deep Mn band (~2eV away from E_C) is expected to be completely filled (or compensated) with electrons leaving no available holes to mediate the magnetic exchange interaction. This results in nonmagnetic behavior as shown in figure 2d. Reducing the silane flow by an order of magnitude moves the Fermi level closer to the Mn energy band. This results in two effects: 1) the electron concentration in E_C is reduced and the film resistivity increases; 2) E_F moves closer to the Mn energy band which becomes partially filled since [Si] « [Mn], and

ferromagnetic behavior results as shown in figures 2 b and 2c.

Mg doping of GaMnN can further confirm the above explanation. A similar trend in magnetic behavior was observed by varying the Mg concentration within GaMnN:Mg films. Figure 3 shows the magnetization curves obtained by SQUID measurements for several GaMnN:Mg samples. The Mg concentration for the samples shown in figure 3 was controlled by varying the (CP_2Mg) partial pressure during growth. The Mg doping concentrations are $5x10^{19}$ and $2x10^{20}$ atoms/cm^3 for samples e and f, respectively. From figure 3, it is apparent that ferromagnetic behavior is diminished because of doping with Mg of these concentrations under these growth conditions as shown in figures 3e and 3f. Hall data for the GaMnN:Mg and the as-grown GaN:Mg samples showed high resistivity, and we could not determine the background hole concentration for these films. Both Mg and Mn atoms form deep acceptor levels of about 0.15eV and 1.4eV above E_V, respectively. Due to their high activation energies, the probability of creating holes at room temperature is minimal for Mg and almost zero for Mn. The [Mn] ≅ [Mg] for the samples used in this study which causes E_F to be located between Mg and Mn energy levels, resulting in a completely empty Mn band and paramagnetic behavior as shown in figures 3 e and 3f.

Figure 4 shows saturation magnetization of GaMnN:Si, GaMnN, and GaMnN:Mg as a function of effective dopant concentration; summarizing the results for this study. At high Mg concentrations, E_F lies closer to the valence and the magnetic behavior diminishes. The same phenomenon occurs when increasing the Si concentration, except E_F is closer to the conduction band. Reducing the amount of these dopants enhances the magnetic properties as shown in figure 4. This clearly demonstrates the role of the Fermi level location on the magnetic properties of these films. These findings exclude any potential confusion that the magnetic properties originate from a gas phase reaction due to the organo-metalic Mn source. Since all these GaMnN films were grown under exactly the same Mn flow, we conclude that the ferromagnetic properties of the GaMnN are not related to secondary phases, precipitates or magnetic clusters.

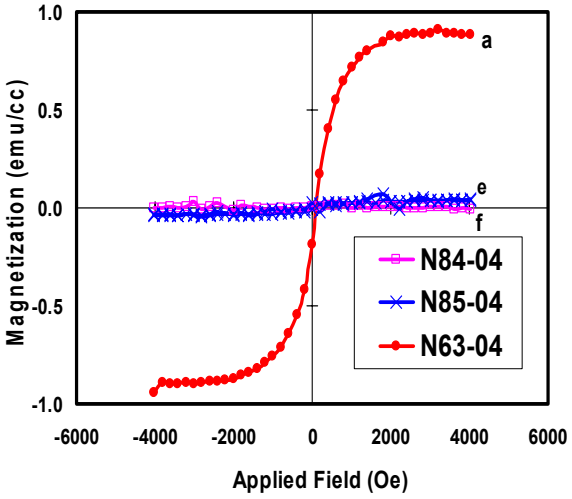

Fig. 3. The effect of Mg concentration on the magnetic properties of GaMnN:Mg; keeping the Mn concentration at 10^{20} atoms/cm^3. SQUID measurements for (a) GaMnN-undoped, (e) GaMnN:Mg ([Mg]= $5x10^{19}$ atoms/cm^3), (f) GaMnN:Mg ([Mg]=$1x10^{20}$ atoms/cm^3).

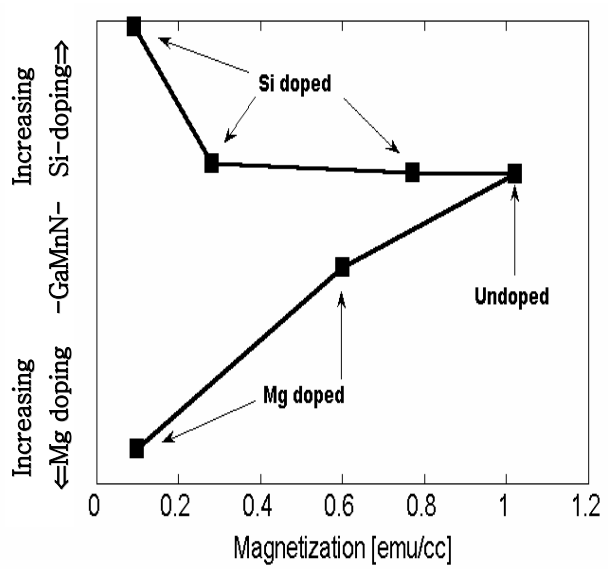

Fig. 4. Figure 4 shows saturation magnetization of GaMnN:Si, GaMnN, and GaMnN:Mg as a function of effective dopant concentration. The magnetic properties are enhanced as the effective dopant concentrations are reduced, i.e. E_F moves closer to the Mn energy band.

3.2 Charge Transfer

In order to study the dependence of GaMnN's magnetic properties on charge transfer, growth conditions rendering GaMnN initially nonmagnetic are selected. We attempt to render these films ferromagnetic via charge transfer across a GaMnN/GaN:Mg interface. The underlying assumption is that the GaMnN films are initially nonmagnetic because the Mn acceptor states are completely filled. Ferromagnetism can be regained by transferring some of the offending electrons in the GaMnN's Mn impurity band into the *p*-type GaN. The Mn concentration in all of these films was found to be 10^{20}/cm^3. In this study, two types of heterojunctions were grown to study the effect of charge transfer on the

magnetic properties; each of which is discussed in detail below.

Structure A is a single heterojunction (SHS) consisting of GaMnN/GaN:Mg grown on an insulating GaN template. The GaN:Mg layer thickness is varied from 0.15 to 0.75 μm, whereas the GaMnN layer is kept constant at 0.375 μm. As the thickness of the *p*-type GaN is increased, the GaMnN's saturation magnetization increases initially and then plateaus at 0.4 μm of GaN:Mg growth as shown in figure 5a. The GaN:Mg heterojunction provides acceptor states that allow charge transfer between the GaMnN and GaN:Mg as required by the equilibration of the Fermi energy within the material. With no *p*-type GaN, the films are non-ferromagnetic, but as the thickness of the GaN:Mg layer increases the GaMnN film becomes ferromagnetic. Further increases of the *p*-type layer thickness beyond 0.4 μm have little to no strengthening effect of the saturation magnetization of the GaMnN films. Figure 5b shows the full hysteresis curves of Structure A at room temperature. Again, note the sharp increase in ferromagnetic strength when the GaMnN forms a heterojunction with 0.15 μm or more of GaN:Mg. To explain these observations, recall that the Mg acceptor level in GaN:Mg is barely activated, only ~1% is ionized. This gives a hole concentration in the low $10^{17}/cm^3$ range leaving the remaining acceptor levels ($\sim 10^{19}/cm^3$) unoccupied. Therefore, for the GaMnN/GaN:Mg SHS (structure A) electrons in the completely filled Mn energy band of the GaMnN layer will transfer into the empty acceptor states in the adjacent *p*-type GaN, resulting in a partially filled Mn energy band. This partially filled Mn energy band satisfies the required conditions to mediate ferromagnetism in these GaMnN/GaN:Mg SHS. Therefore, these films will be ferromagnetic with the magnitude of the saturation magnetization depending on the availability of unoccupied Mg acceptor states as well as the thickness of the GaN:Mg layer as shown in figure 5. The carrier transfer process will continue until a built-in field and a depletion layer are established at the GaMnN/GaN:Mg interface.

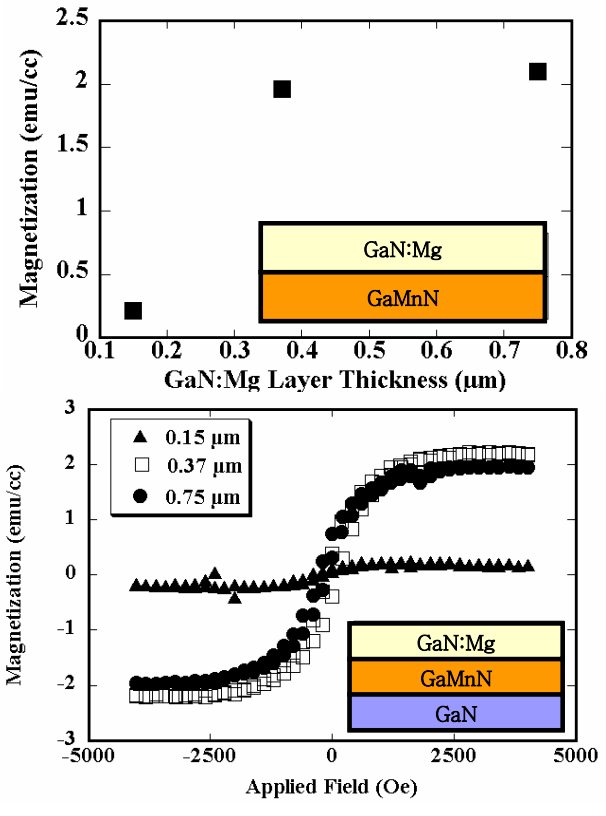

Fig. 5. (a) Saturation magnetization as a function of the GaN:Mg layer thickness for structure A; (b) SQUID measurements for GaN:Mg = 0.15, 0.37, and 0.75 μm. Note the GaMnN layer is 0.37 μm for these samples. GaMnN/GaN:Mg SHS shown in insets.

Structure B is GaN:Mg/AlGaN/GaMnN/AlGaN /GaN:Mg multilayer structures (MLS) with the AlGaN layers serving as a wide band gap barrier for the carriers. The thickness and composition of the GaN:Mg (0.75 μm) and GaMnN (0.375 μm) layers were selected such that in the absence AlGaN the resulting films would be ferromagnetic, as determined from the study on structure A. The AlGaN barrier thickness, t_b, was varied from 25 to

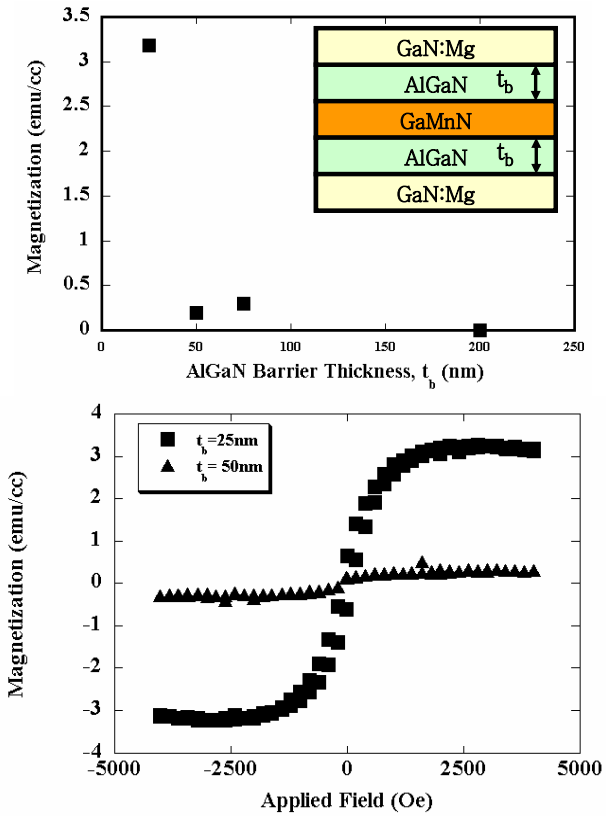

Fig. 6. (a) Saturation magnetization as a function of AlGaN barrier thickness for GaN:Mg/AlGaN/GaMnN /AlGaN/GaN:Mg MLS. (b) SQUID measurements at room temperature for the multilayer structures.

200 nm with a constant Al concentration of 30%. As the thickness of the AlGaN barrier is increased beyond 25 nm, the GaMnN's saturation magnetization decreases sharply as shown in figure 6a. SQUID data indicates that the GaMnN films are ferromagnetic only for very thin AlGaN barriers (t_b ≤25nm) and are non-ferromagnetic for thicker AlGaN barriers as shown in figure 6b. Carrier transfer across the barrier will take place by either tunneling or thermionic emission. The probability of tunneling will exponentially decay with the AlGaN barrier thickness (t_b). For very thin AlGaN barriers (t_b <25nm) the charge transfer across the GaMnN/GaN:Mg interface is not impeded and ferromagnetic properties are retained. This situation is very similar to the findings for structure A, where the *p*-type heterojunction provides acceptor states that allow charge transfer between the GaMnN and GaN:Mg. However, in the case of t_b>50nm, the charge transfer across the GaMnN/GaN:Mg interface is highly impeded and the ferromagnetic properties are very weak or no longer detected. In this situation, the electrons within the GaMnN cannot be depleted which leaves the Mn energy band filled, thus preventing the Mn-Mn ferromagnetic exchange interaction.

Both structures A and B indicate that a partially filled Mn energy level is required to mediate the magnetic exchange interaction. This was demonstrated via charge transfer across a GaMnN/GaN:Mg interface. These findings also exclude any potential confusion that the magnetic property originate from a gas phase reaction due to the organo-metallic Mn source, secondary phases, clustering, or precipitates.

3.3 Devices

Devices grown for this study consist of *n*-GaN:Si/ *i*-GaMnN/*p*-GaN:Mg layers grown by MOCVD. The GaMnN layer is approximately 0.1 – 0.2 µm thick with up to 1% Mn. Two types of structures were grown: 1) devices where the *p*-layer is grown first (*p*-down) and 2) *n*-layer was deposited first (*n*-down). A control *p-n* junction was also grown for comparison. The device pattern designed for this study consisted of interdigitated fingers with a footprint of 400 µm x 400 µm as shown in figure 7. The device Mesas were etched to a depth of ~1.4 µm using a Trion Technology ICP-RIE plasma chamber at 5 mTorr with a BCl_3/Cl_2 gas chemistry with 400W of ICP power and 150W of RIE power. The following metallization schemes were deposited using a Thermionics e-beam evaporator: Ti(200Å)/ Al(2000Å)/Ti (400Å)/Au(500Å) for the *n*-type contact, and Ni(200Å)/Au(2000Å) for the *p*-type contact.

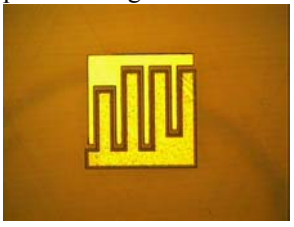

Fig. 7. Fabricated *p-i-n* device.

The growth temperature (1000°C) and Mn:Ga partial pressure ratio for the GaMnN layer was the same for all *p-i-n* devices studied. Mn concentration within the devices is ~0.5%, as determined by SIMS measurements. The carrier concentrations for the *n* and *p*-type layers in the *p-i-n* devices are ~ $5x10^{18}/cm^3$ and $1x10^{18}/cm^3$ respectively. Room temperature SQUID measurements for the *p-i-n* devices are shown in figure 4a and b for samples N044 (*p*-down) and N047 (*n*-down), respectively. SQUID measurements were performed on samples where Pd(200Å)/Au(1500Å) was used as the non-magnetic *p*-type contacts. The GaMnN *i* layer for sample N044-04 is ~0.2µm thick whereas N047 has a thickness of ~0.45µm. Figure 8 shows that the saturation magnetization for both samples is ~1.25 emu/cc, indicating these growth conditions for creating magnetic GaMnN are reproducible.

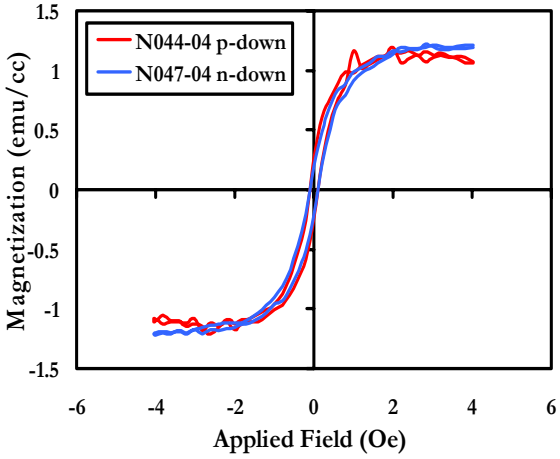

Fig. 8. Magnetization curves for N044 and N047 at 300K.

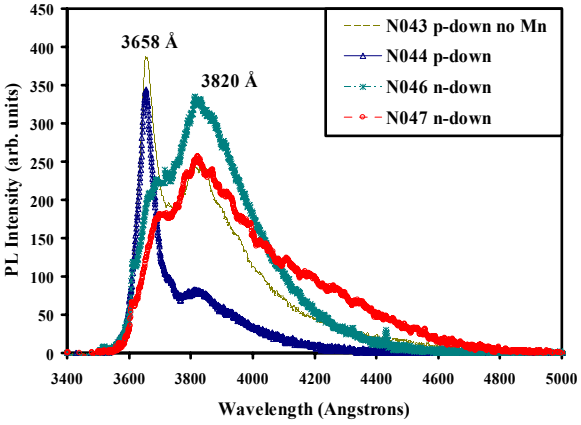

Fig. 9. Photoluminescence measurements of *p-i-n* devices, showing emission at 365 nm and 382nm.

Figure 9 shows the photoluminescence measurements performed on the *p-i-n* devices. For the *p*-down samples N043 and N044, PL emissions centered at 365nm and 382 nm are observed. These peaks originate from the *n*-type and *p*-type layers, respectively. However, for *n*-down samples N046 and N047 only emission from the *p*-type layer at 382 nm is observed. Transitions to the Mn energy band cannot be observed using this experimental setup. Future experiments will focus on the Mn transitions.

I/V characteristics of the devices under forward and reverse bias are shown in figure 10a and 10b, respectively. The series resistance is higher in the samples with *p*-down as compared to the *n*-down devices as seen in figure 10a due to the low mobility of holes. The Mn-doped device N044 has a lower series resistance than the undoped *p-n* diode N043 (*p*-down). However, sample N044 also exhibits a lower breakdown voltage under reverse bias conditions (figure 10b) indicating the lower series resistance is from leakage current. The lower series resistance observed in sample N047-04 is attributed to having the higher mobility *n*-layer down. Figure 11 shows the electroluminescence for several *p-i-n* samples. In these the samples, the predominant emission wavelength are 400-430 nm indicating that recombination is occurring in the *p*-GaN layer. Further analysis on the polarization state of the light emitted from these devices still needs to be performed.

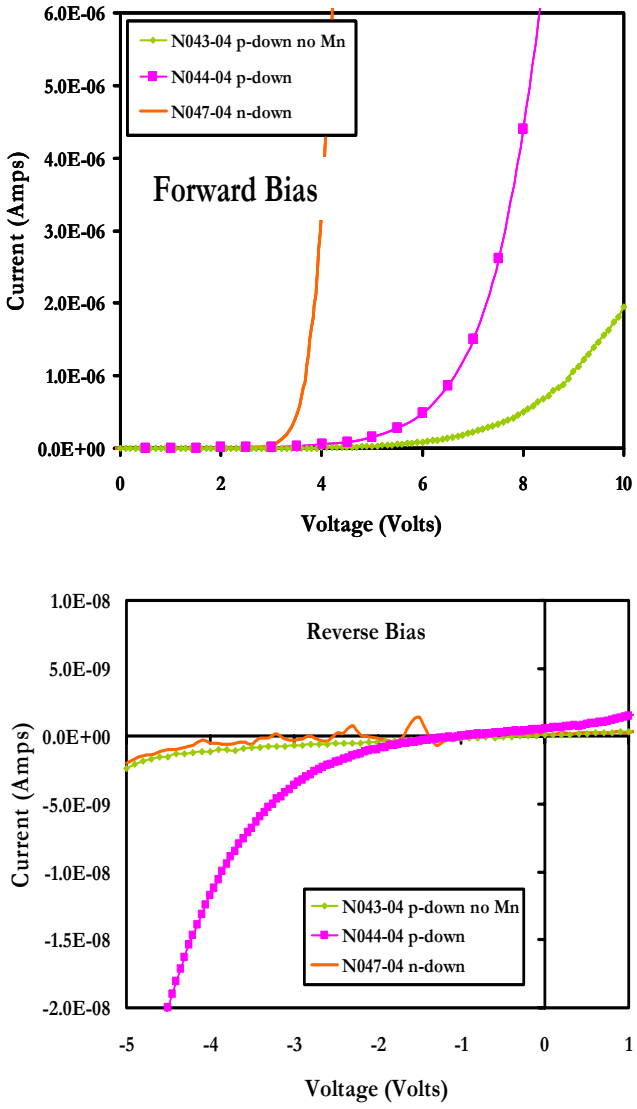

Fig. 10. I/V characteristics of the *p-i-n* devices for (a) forward bias and (b) reverse bias.

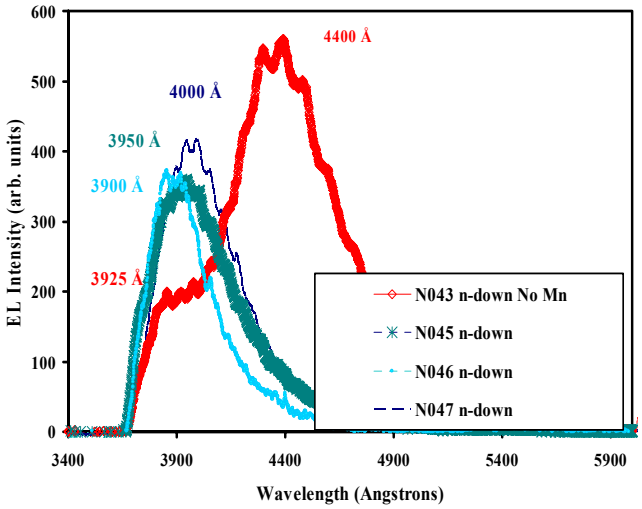

Fig. 11. Shows the electroluminescence for samples N043, N045, N046 and N047.

CONCLUSIONS

In conclusion, we were able to demonstrate that the magnetic properties of GaMnN films depend on the position of the Fermi level, which can be altered by Mg or Si doping. When the Fermi level lies within or close to the Mn impurity band there is partial occupancy of electrons and holes in this Mn impurity band, and ferromagnetic behavior is achieved. This was further confirmed by charge transfer across the GaMnN/GaN:Mg interface. It was demonstrated by depleting carriers from the GaMnN layer that the ferromagnetic properties are enhanced. Several *p-i-n* devices were grown and fabricated. The magnetic properties of these devices were maintained after processing. Additionally, photoluminescence and electroluminescence measurements revealed emission spectra characteristic of GaN *p-n* junctions. The current results exclude the presence of precipitants or clusters as the origin of the observed room temperature magnetic properties in the MOCVD grown GaMnN films.

ACKNOWLEDGEMENTS

This work is supported by the Army Research Office.

REFERENCES

Dietl, T., Sawicki, M., Khoi, L. v., Jaroszynski, J.,Kossacki, P., Cibert, J., Ferrand, D., Tatarenko, S., and Wasiela, A., *Physica Status Solidi B-Basic Research* **229,** 665-672 (2002).

Fiederling, R., Keim, M., Reuscher, G., Ossau, W., Schmidt, G., Waag, A. and Molenkamp, L.W., *Nature* **402,** 787-790 (1999).

Hori*, Journal of Applied Physics,* **91,** 7911-7913 (2002).

Korotkov, R.Y., Gregie, J.M., Wessels, B.W., *Appl. Phys. Lett*. **80**, 1731 (2002).

Koshihara, S., Oiwa, A., Hirasawa, M., Katsumoto , S., Iye, Y,. Urano, C, Takagi, H., and Munekata, H., *Phys. Rev. Lett.* **78**, 4617 (1997).

Ohno, H., Shen, A., Matsukura, F., Oiwa, A., Endo, A., Katsumoto, S., and Iye, Y., *Applied Physics Letters* **69,** 363-365 (1996).

Ohno, H., *Science* **281**, 951 (1998).

Reed, M.L., El-Masry, N.A., Stadelmaier, H.H., Ritums, M.K., Reed, M.J., Parker, C.A., Roberts, J.C., and Bedair, S.M., *Applied Physics Letters* **79,** 3473-3475 (2001).

Reed, M.L., Berkman, E.A., Reed, M.J., Arkun, F.E., Chikyow, T., Bedair, S.M., Zavada, J.M., and El-Masry, N.A., *Mat. Res. Soc. Symp.* Proc. Vol. 798, Y.8.6.1 (2004).

Thaler, G.T., Overberg, M.E., Gila, B., Frazier, R., Abernathy, C.R., Pearton, S.J., Lee, J.S., Lee, S.Y., Park, Y.D., Khim, Z.G., Kim, J., and Ren, F., *Applied Physics Letters* **80,** 3964-3966 (2002).

Thaler, G., Frazier, R., Gila, B. Stapelton, ,J., Davidson, M. , Abernathy, C.R., Pearton, S.J., Serge, C., *Appl. Phys. Lett.* **84**, 2578 (2004).

Sonoda, S., Hori, H., Yamamoto, Y., Sasaki, T., Sato, M., Shimizu, S., Suga, K,. and Kindo, K., *Ieee Transactions on Magnetics* **38,** 2859-2862 (2002).

Sonoda, S., Shimizu, S., Sasaki, T., Yamamoto Y., and Hori, H., *J. Cryst. Growth*, **237-239**, 1358 (2002).